

A volumetric conformal mapping approach for clustering white matter fibers in the brain

Vikash Gupta¹, Gautam Prasad², and Paul Thompson¹

¹ Imaging Genetics Center, University of Southern California

² Google Inc., Los Angeles

Abstract. The human brain may be considered as a genus-0 shape, topologically equivalent to a sphere. Various methods have been used in the past to transform the brain surface to that of a sphere using harmonic energy minimization methods used for cortical surface matching. However, very few methods have studied volumetric parameterization of the brain using a spherical embedding. Volumetric parameterization is typically used for complicated geometric problems like shape matching, morphing and isogeometric analysis. Using conformal mapping techniques, we can establish a bijective mapping between the brain and the topologically equivalent sphere. Our hypothesis is that shape analysis problems are simplified when the shape is defined in an intrinsic coordinate system. Our goal is to establish such a coordinate system for the brain. The efficacy of the method is demonstrated with a white matter clustering problem. Initial results show promise for future investigation in these parameterization technique and its application to other problems related to computational anatomy like registration and segmentation.

Keywords: Conformal mapping, Volumetric Parameterization, Spectral clustering, White matter fiber clustering.

1 Introduction

Shape parameterization is a well researched area in the computational geometry community [1,2]. In computational anatomy, many algorithms have been devoted to surface parameterization [3–6] and its applications to cortical surface matching and registration [7]. Shi et. al [8] used conformal mapping between the cortical surfaces for cortical label fusion. Brain Transfer [9] is a recent method suggested by Lombaert et. al is used to find correspondences between cortical surface across subjects as well as functional areas. Surface parameterization may be sufficient for analyzing surface geometry. However, it falls short when there is significant information contained inside the shape under consideration (brain). Here we developed a parameterization technique that parameterizes the entire volume of the brain and every structure contained in it. Thus, cortical surface parameterization is in fact a byproduct of this method.

Following work by Wang, Yau and colleagues [10] using "sphere carving" to harmonically map the brain to a sphere, a bijective mapping between the brain

and the topologically equivalent sphere can be established using a 3D harmonic function. Such a parameterization gives us a coordinate system intrinsic to the brain shape, which may simplify various sub-problems related to computational anatomy such as registration, segmentation and automated clustering of white matter fibers. We will show a potential application of this parameterization technique, to assist with automated clustering of white matter fibers.

White matter fibers serve as neural pathways that connect different parts of the brain. Diffusion weighted imaging (DWI) and tractography are used to study the white matter organization in the brain. Clustering the white matter fibers is an important step towards statistical analyses. One commonly used clustering method [11] uses manual ROI delineation on the FA images. These regions can be used to seed whole-brain fiber tractography, which is then grouped into white matter bundles using spectral clustering. One method used Hausdorff's distance [12] as a distance metric between two fibers. Another more recent method for fiber clustering was proposed by [13]. In this method, each fiber is represented using Gaussian mixture models followed by a hierarchical total Bregman soft clustering. The authors [14] provide a more complete overview of different clustering techniques.

In this paper, we use the proposed conformal mapping technique to parameterize the white matter tracks. We then use a hierarchical spectral clustering approach to classify a given set of tracks into individual anatomically relevant fiber bundles. The proposed method does not rely on any tractography atlas or region of interest (ROI) information. The accuracy of the method is compared with manual clustering results.

2 Conformal Mapping: A Heat Transfer Analogy

To understand the volumetric parameterization problem addressed in this paper, we draw an analogy between our problem and the heat transfer problem in solid bodies. For the purpose of explanation, consider a solid body is maintained at a constant high temperature on the surface and at another point inside the brain at a constant low temperature. At steady state a thermal gradient will be set up between the surface and the center with different layers of isothermal surfaces. The heat from the high temperature surface is conducted towards the center through heat-flow lines. These heat-flow lines intersect the isothermal surfaces at right angles. We use this property to define a coordinate system for the whole brain. We refer to the fixed low temperature point as the *shapecenter* and the temperature field as ϕ .

3 Harmonic Function

The harmonic function is a C^2 continuous function that satisfies Laplace's equation. It is used to establish a bijective mapping between the brain and the topologically equivalent spherical shape. If $\phi : U \rightarrow \mathbb{R}^n$, where $U \subseteq \mathbb{R}^n$ is some domain and ϕ is some function defined over U , the function ϕ is harmonic if its Laplacian

vanishes over U , i.e., $\nabla^2\phi = 0$. In terms of Cartesian coordinate system, we can write

$$\nabla^2\phi = \sum_{i=1}^n \frac{\partial^2\phi}{\partial^2x_i} = 0 \quad (1)$$

where x_i is the i^{th} Cartesian coordinate and n is the number of dimensions of the shape under study (here, 3). The harmonic function has two properties called the mean value and the maximum principle property, which are important for the parameterization problem being discussed.

3.1 Mean Value property

If a ball $B(x, r)$ with center x and radius r is completely contained within the domain under study, then the value of the harmonic function $\phi(x)$ is given by the average values of the function over the surface of the sphere. This average value is also equal to the average values of ϕ inside the sphere.

3.2 Maximum principle

According to the maximum principle, the harmonic function ϕ cannot have local extrema within the domain U . The Laplacian of the harmonic functions should be zero by definition. For a local extremum to exist all the components of the second order partial derivatives of the function should have the same sign. If all of them have the same sign, their sum will never be zero and thus they will never be able to satisfy Laplace's equation.

4 Algorithm

For the parameterization method, the volume generated by the fractional anisotropy (FA) mask is used. Image voxels were classified as either boundary surface points or internal points. For every subject the inferior end of the fornix on the mid-line was located manually and designated as the "shape center". In the future, more automated approach towards choosing the same will be investigated and adopted.

4.1 Boundary Conditions

We apply the Dirchlet boundary conditions for the shapecenter and the boundary surface, i.e., we fix the value of the function ϕ on all the boundary nodes and the shapecenter to 1 and 0 respectively. All the remaining points are assigned random values between 0 and 1 as the initial condition.

4.2 Potential Computation

An iterative finite difference scheme is used to solve the Laplace equations. If $\phi(x, y, z)$ is a harmonic function, its second derivative is computed using the Taylor's series expansion.

$$\frac{\partial^2 \phi}{\partial x^2} = \frac{\phi(x_{i-1}, y_i, z_i) - 2\phi(x_i, y_i, z_i) + \phi(x_{i+1}, y_i, z_i)}{h^2} \quad (2)$$

$$\frac{\partial^2 \phi}{\partial y^2} = \frac{\phi(x_i, y_{i-1}, z_i) - 2\phi(x_i, y_i, z_i) + \phi(x_i, y_{i+1}, z_i)}{k^2} \quad (3)$$

$$\frac{\partial^2 \phi}{\partial z^2} = \frac{\phi(x_i, y_i, z_{i-1}) - 2\phi(x_i, y_i, z_i) + \phi(x_i, y_i, z_{i+1})}{l^2} \quad (4)$$

where h, k and l are the step sizes in the x, y and z directions respectively. Using the Laplace equation from 1 we have

$$\begin{aligned} \phi(x_i, y_i, z_i) &= \frac{\phi(x_{i+1}, y_i, z_i) + \phi(x_{i-1}, y_i, z_i)}{6h^2} \\ &+ \frac{\phi(x_i, y_{i-1}, z_i) + \phi(x_i, y_{i+1}, z_i)}{6k^2} + \frac{\phi(x_i, y_i, z_{i-1}) + \phi(x_i, y_i, z_{i+1})}{6l^2} \end{aligned}$$

The above potential values are computed until the maximum difference between two successive iterations is below a certain threshold ζ . Generally, ζ is chosen to be 10^{-12} .

4.3 Computing heat-flow lines

Streamlines or the heat flow lines are orthogonal to the isothermal (equipotential) surfaces. Each of the streamlines starts from the boundary points on the brain surface and progresses towards the designated shapecenter. Each of these streamlines approaches the shapecenter at unique angle(s), which remain constant along the streamline. This property is endowed by construction. The streamlines are computed by solving the following differential equation,

$$\frac{\partial X}{\partial t} = -\eta \nabla \phi[X(t)] \quad (5)$$

where $X = [x, y, z]^T$ is the coordinate vector and η is the normalization constant. MATLAB's (version R2014b) *ode23* routine is used to solve the system of differential equations. The differential equation solver requires the potential values at the non-grid points within the domain U . The intermediate values are interpolated from the neighboring grid points using a local bilinear fitting model as,

$$\phi(x, y, z) = p_1xyz + p_2xy + p_3yz + p_4zx + p_5x + p_6y + p_7z + p_8 \quad (6)$$

where p_i 's are constants. Eight neighborhood grid points are used to calculate the p_i 's and these are used to interpolate the ϕ at a non-grid point using the above equation.

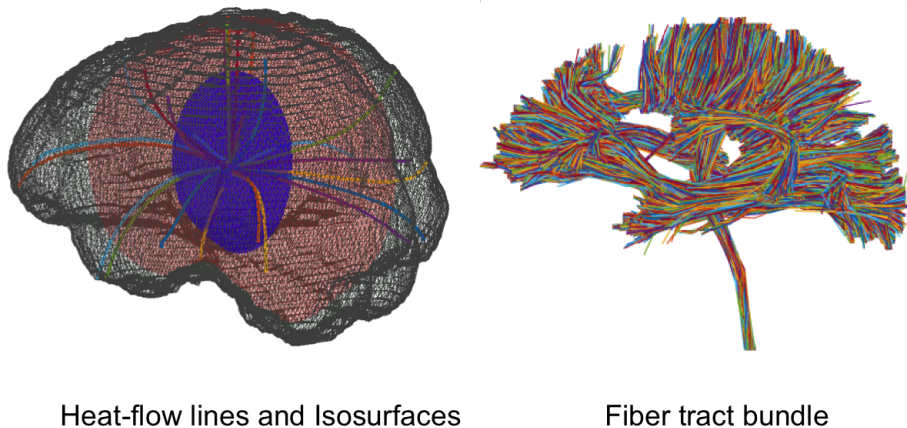


Fig. 1. Left: 3D view of different equipotential surfaces are shown. The heat-flow lines emanating from the surface approach the shapecenter at unique polar and azimuthal angles. These angles remain constant along the streamlines, intersect the surfaces at right angles. **Right:** The white matter fibers to be classified into different groups.

4.4 Parameterizing the Brain

Each streamline originating from each of the boundary points approaches the shapecenter at a unique angle. These angles remain constant along the streamlines. In case of three dimensional objects the angle of approach is characterized by the elevation (θ) and the azimuthal (ψ) angles. The vector between the shapecenter and the end point of the streamline is calculated. The angles are calculated using the Cartesian to spherical coordinate transformation

$$\psi = \text{atan2}(y, x); \quad \theta = \text{atan2}(\sqrt{x^2 + y^2}, z) \quad (7)$$

The streamlines intersect the equipotential surfaces at right angles (see figure 1). Each point of intersection generates a tuple $[\phi, \theta, \psi]^T$ for the corresponding Cartesian coordinates $[x, y, z]^T$.

5 Mapping the White Matter Fibers

After the whole brain is parameterized as mentioned above, each fiber tract is mapped to the new coordinate system, i.e., in the spherical space. At this stage, we have a bijective mapping between the Cartesian coordinates of every voxel in the brain and the newly computed coordinate system. A KD-tree structure is built using the native brain coordinates for ϕ , θ and ψ . For every point on the fiber streamline, the algorithm searches for ten neighborhood points and computes a weighted average to get the corresponding coordinate in the target domain. This process establishes the mapping of fibers in the target domain.

6 Clustering White Matter Fibers

6.1 Tracking white matter fibers

Data was obtained from Alzheimer’s Disease Neuorimaging Initiative for the Department of Defense (ADNI-DoD). For each of the DTI images, 46 volumes were acquired with 5 T2 weighted B0 volumes and 41 diffusion-weighted volumes with voxel size of $1.36 \times 1.36 \times 2.7 \text{ mm}^3$. The scans were acquired using a GE 3.0T scanner, using echo planar imaging with parameters: TR/TE = 9050/62 ms. Images were corrected for eddy-current distortions and skull-stripped. The diffusion gradient vectors are rotated based on the matrix transformation resulting from eddy-current correction. Whole-brain tractography was performed with Camino (<http://cmic.cs.ucl.ac.uk/camino/>), an open source software package that uses either streamline or probabilistic methods to reconstruct fiber paths. We performed fiber a probabilistic algorithm, called the ‘Probabilistic Index of Connectivity’ (PICO) in Camino [15]. Seed points were chosen at those voxels whose FA values were greater than 0.2. Monte Carlo simulation was used to generate fibers proceeding from the seed points throughout the entire brain [16]. Streamline fiber tracing followed the voxel-wise PDF profile with the Euler interpolation method for 7 iterations per each seed point. The maximum fiber turning angle was set to 60 degree/voxel, and tracing stopped at any voxel whose FA was less than 0.2.

For the purpose of comparison against the ground truth, manual labeling was performed by experts in neuroanatomy. Essentially, the FA images of these subjects were registered to a single-subject template in the ICBM-152 space called the “Type II Eve Atlas” (a 32-year-old healthy female) [17]. The entire brain of the “Eve” template was parcellated using 130 bilateral ROIs [18]. The labeled template ROIs were re-assigned to both subjects by warping them with the deformation fields generated by Advanced Neuroimaging Tools (ANTs) [19]. Each tract was manually edited to remove visible outliers. For each tract, there is a certain set of ROIs that it intersects – a fiber must traverse all the required ROIs for a given tract to be considered, otherwise the fiber was discarded.

6.2 Unsupervised clustering of white matter fibers

Various atlas based fiber clustering techniques are being used widely [20, 21]. However, in our knowledge a completely automated fiber clustering method is non-existent. The authors in [11] claim that the presented method is automatic. However, the method requires manual region of interest labeling for seeding the fiber tractography algorithms. Manual delineation can be a time consuming and laborious process, and does not provide a fully automated method. Furthermore, the robustness of the clustering algorithm under a whole brain tractography can be varied depending on the skill and expertise of the labeler.

Spectral Clustering is one of the widely used unsupervised clustering methods. The details of the method are available in [22, 23]. A spectral clustering method requires a similarity criterion (or a distance metric) to be defined. This

distance metric is used to compare all the N fibers with each other to create the affinity matrix of size $N \times N$. The idea behind spectral clustering is to approximate the affinity matrix based on its largest eigenvalues. If k eigenvalues are chosen, it implies that the data is distributed in a space spanned by the corresponding k eigenvectors. Here we choose k as the same as expected number of clusters.

Before clustering can be performed on the white matter tracts, the fiber tracts need to be pre-processed. These pre-processing steps are crucial for good clustering results. All the white matter fibers are reparameterized using the arc length to contain the same number of points. The resampled tracks are mapped into the spherical domain as mentioned in section 5. At this point, for each Cartesian coordinate $[x, y, z]$ on the track we have an equivalent coordinate $[\phi, \theta, \psi]$ in the spherical domain. The distance metric (d_{ij}) used for constructing the affinity matrix is defined as sum of squared differences on the new mapped coordinates. Thus, if i and j are two fibers and N is the total number of points in a track.

$$d_{ij} = \sum_{k=1}^N (p_i^k - p_j^k)^2$$

where p_i^k is one of the coordinates, i.e., ϕ , θ or ψ of the k^{th} point in the fiber i . The hierarchical clustering is performed in this set of parameterized coordinates. The steps involved are enumerated as follows:

1. The mid-sagittal plane is located using the fractional anisotropy (FA) image and the white matter fibers are separated into the left and right hemispheres.
2. Corpus callosum is contained in both the hemispheres. Thus, it can be segmented by performing a logical AND operation on the two sets of fiber tracks obtained in the previous step.
3. An estimated desired number of clusters is provided by the user.
4. Spectral clustering is performed on ϕ coordinates of the tracks.
5. The mean variance of each of the clusters obtained is calculated. It is understood that if a group contains only one cluster, the mean variance will be low (typically < 40).
6. The clusters with variance above the desired threshold is inspected and spectral clustering is performed again using the azimuthal angles (θ) of the tracks.
7. The previous step is repeated again and if there are mis-classified tracks another clustering is performed using the elevation angle ψ .
8. Because of the hierarchical nature of the clustering, we will generally end up with over-classification, i.e., we get more groups of fibers than desired.
9. The over classified clusters are merged. Each cluster is merged with those of the remaining ones and the resulting variance is calculated. If the variance is lower than the threshold, the clusters are merged. The process continues as long as there are more clusters than desired by the user.

The steps 4-7 in the algorithm is schematically represented in figure 2. Similar process is repeated for the right hemisphere.

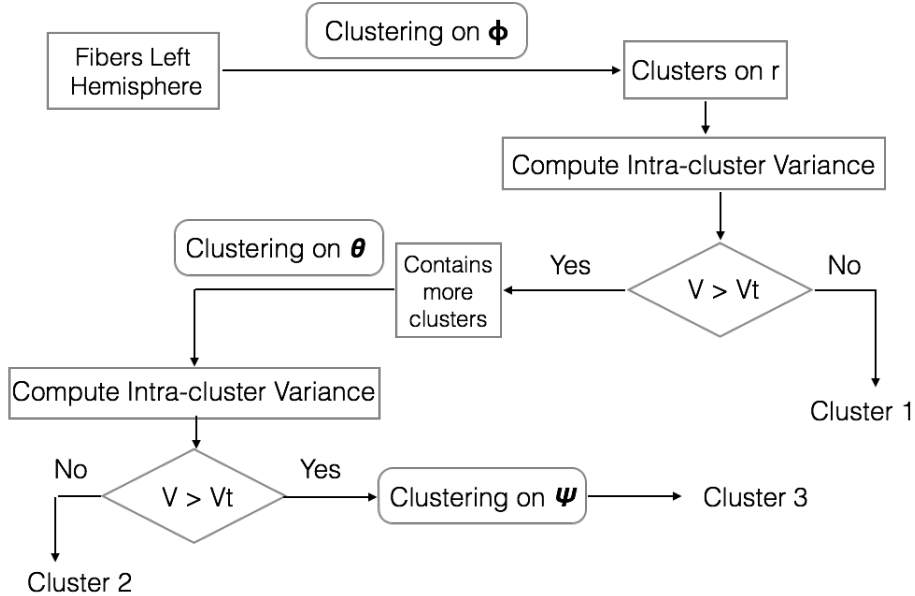


Fig. 2. The different steps in the hierarchical clustering process (steps 4-7) are shown. V represents the mean intra-cluster variance and V_t represents the variance threshold. Cluster 1, 2 and 3 represents the clusters obtained at each step of the process.

6.3 Results of clustering

In figure 3, we show the results of the proposed hierarchical clustering. The left column shows the results of first level of clustering, i.e., with r co-ordinate. The tracks are overlaid on the corresponding FA image for anatomical reference. The variance of the cluster is mentioned below each panel. As expected, we found that the variance of the clusters containing a single group is comparatively lower than the ones which contained more than one groups. The groups with variance higher than 40 (threshold) were re-clustered as shown but with different coordinates until the variance is lower than the variance threshold. At this point we do have more sub-clusters than expected. We follow an agglomerative approach for combining the redundant clusters. The hierarchical nature of the method makes the clustering process tractable. For the purpose of validation, a ground truth data set was generated using manual labeling. A comparison between the proposed clustering method and the traditional spectral clustering method using Hausdroff distance as metric is shown. When compared to the ground truth the proposed method is able to retrieve all the fiber bundles as see in figure 4.

7 Conclusion and Future Work

In this paper we proposed a novel volumetric parameterization technique for parameterizing the brain to a sphere. Unlike prior methods which generally rely

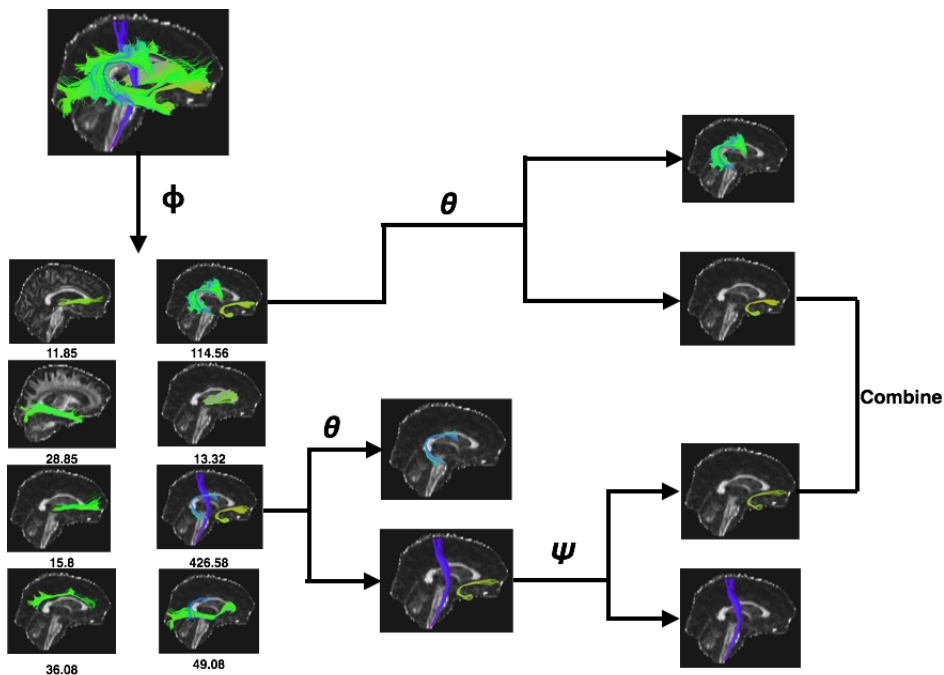


Fig. 3. The left column shows the result of clustering based on the ϕ coordinate. In the second column, two of the fiber bundles can be further classified. A second and third level of clustering is performed based of the azimuthal θ and polar ψ angles. At this stage, we have some over classified bundles as seen in the last column. The bundles with the combined variance less than a user defined threshold are combined.

on surface parameterization, the method presented in this paper parameterizes the whole brain, following early work by [10]. This method may be useful for developing novel shape based-registration methods, mapping regions of interest, performing brain connectivity analysis and white matter fiber clustering. We have also shown a potential use of the method in clustering white matter tracts. The presented clustering method does not require any ROI based seeding or image registration. The fiber tractography as well as the clustering was performed in the native space of diffusion acquisition. In the present implementation of the method the shape-center is chosen manually. However, in the future the shapecenter can be chosen automatically, preferably at the anterior or posterior commissure and can be located automatically using tools such as FreeSurfer. We compared our results with spectral clustering methods using Hausdroff distance and showed that the proposed method out-performs the former. The method has to be tested for robustness against noisy data. In the future, we would like to use the method for statistical analysis on large datasets for comparing fiber tract

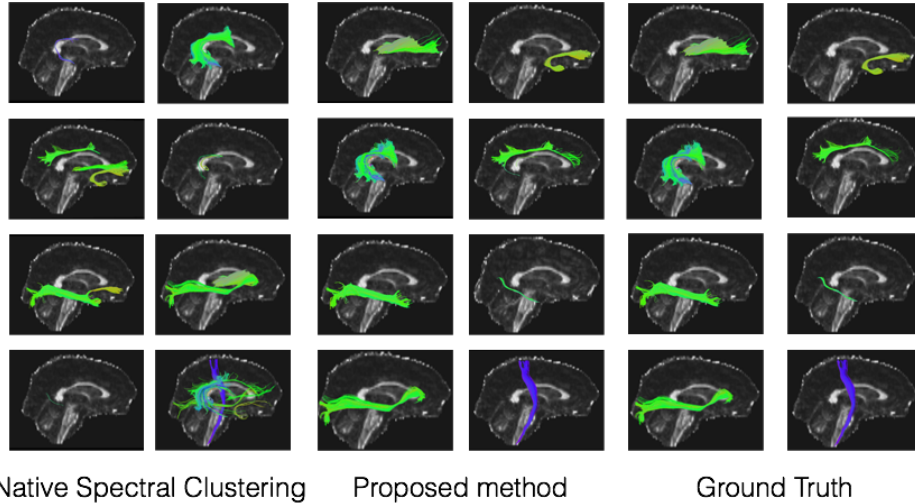


Fig. 4. A comparison between the clustering methods. The manual segmentation is shown in the right most column. The left and the right columns show spectral clustering using the Hausdroff distance and the proposed method respectively.

geometries. We believe that, a method which solely relies on the subject data and not on any atlas will be particularly useful for clustering white matter fibers for surgical purposes and in subject with significant white matter deformities that cannot be represented in the white matter atlas.

8 Acknowledgements

This study was supported in part by a Consortium grant (U54 EB020403) from the NIH Institutes contributing to the Big Data to Knowledge (BD2K) Initiative, including the NIBIB. The authors are also thankful to Dr. Ratnesh Kumar from Teradeep Inc., Sunnyvale (California) for valuable insights and suggestions.

References

1. Floater, M.S., Hormann, K.: Surface parameterization: a tutorial and survey. *Advances in multiresolution for geometric modelling* **1**(1) (2005)
2. Gupta, V., Voruganti, H.K., Dasgupta, B.: Domain mapping for volumetric parameterization using harmonic functions. *Computer-Aided Design and Applications* **11**(4) (2014) 426–435
3. Gu, X., Wang, Y., Chan, T.F., Thompson, P.M., Yau, S.T.: Genus zero surface conformal mapping and its application to brain surface mapping. *Medical Imaging, IEEE Transactions on* **23**(8) (2004) 949–958
4. Wang, Y., Gu, X., Chan, T.F., Thompson, P.M., Yau, S.T.: Brain surface conformal parameterization with algebraic functions. In: *Medical Image Computing and Computer-Assisted Intervention–MICCAI 2006*. Springer (2006) 946–954

5. Wang, Y., Shi, J., Yin, X., Gu, X., Chan, T.F., Yau, S.T., Toga, A.W., Thompson, P.M.: Brain surface conformal parameterization with the Ricci flow. *Medical Imaging, IEEE Transactions on* **31**(2) (2012) 251–264
6. Mémoli, F., Sapiro, G., Osher, S.: Solving variational problems and partial differential equations mapping into general target manifolds. *Journal of Computational Physics* **195**(1) (2004) 263–292
7. Gutman, B.A., Madsen, S.K., Toga, A.W., Thompson, P.M.: A family of fast spherical registration algorithms for cortical shapes. In: *Multimodal Brain Image Analysis*. Springer (2013) 246–257
8. Shi, Y., Lai, R., Toga, A.W.: Conformal mapping via metric optimization with application for cortical label fusion. In: *International Conference on Information Processing in Medical Imaging*, Springer (2013) 244–255
9. Lombaert, H., Arcaro, M., Ayache, N.: Brain transfer: Spectral analysis of cortical surfaces and functional maps. In: *International Conference on Information Processing in Medical Imaging*, Springer (2015) 474–487
10. Wang, Y., Gu, X., Chan, T.F., Thompson, P.M., Yau, S.T.: Volumetric harmonic brain mapping. In: *Biomedical Imaging: Nano to Macro, 2004. IEEE International Symposium on*, IEEE (2004) 1275–1278
11. O’Donnell, L., Kubicki, M., Shenton, M.E., Dreusicke, M.H., Grimson, W.E.L., Westin, C.F.: A method for clustering white matter fiber tracts. *American Journal of Neuroradiology* **27**(5) (2006) 1032–1036
12. Corouge, I., Gouttard, S., Gerig, G.: Towards a shape model of white matter fiber bundles using diffusion tensor MRI. In: *Biomedical Imaging: Nano to Macro, 2004. IEEE International Symposium on*, IEEE (2004) 344–347
13. Liu, M., Vemuri, B.C., Deriche, R.: Unsupervised automatic white matter fiber clustering using a gaussian mixture model. In: *Biomedical Imaging (ISBI), 2012 9th IEEE International Symposium on*, IEEE (2012) 522–525
14. Guevara, P., Poupon, C., Rivière, D., Cointepas, Y., Descoteaux, M., Thirion, B., Mangin, J.F.: Robust clustering of massive tractography datasets. *NeuroImage* **54**(3) (2011) 1975–1993
15. Cook, P., Bai, Y., Nedjati-Gilani, S., Seunarine, K., Hall, M., Parker, G., Alexander, D.: Camino: open-source diffusion-mri reconstruction and processing. In: *14th scientific meeting of the international society for magnetic resonance in medicine*. Volume 2759., Seattle WA, USA (2006)
16. Parker, G.J., Alexander, D.C.: Probabilistic monte carlo based mapping of cerebral connections utilising whole-brain crossing fibre information. In: *Biennial International Conference on Information Processing in Medical Imaging*, Springer (2003) 684–695
17. Oishi, K., Faria, A., Jiang, H., Li, X., Akhter, K., Zhang, J., Hsu, J.T., Miller, M.I., van Zijl, P.C., Albert, M., Lyketsos, C.G., Woods, R., Toga, A.W., Pike, G.B., Rosa-Neto, P., Evans, A., Mazziotta, J., Mori, S.: Atlas-based whole brain white matter analysis using large deformation diffeomorphic metric mapping: Application to normal elderly and alzheimer’s disease participants. *NeuroImage* **46**(2) (2009) 486 – 499
18. Zhang, Y., Zhang, J., Oishi, K., Faria, A.V., Jiang, H., Li, X., Akhter, K., Rosa-Neto, P., Pike, G.B., Evans, A., et al.: Atlas-guided tract reconstruction for automated and comprehensive examination of the white matter anatomy. *Neuroimage* **52**(4) (2010) 1289–1301
19. Avants, B.B., Epstein, C.L., Grossman, M., Gee, J.C.: Symmetric diffeomorphic image registration with cross-correlation: evaluating automated labeling of elderly and neurodegenerative brain. *Medical image analysis* **12**(1) (2008) 26–41

20. O'Donnell, L.J., Westin, C.F.: Automatic tractography segmentation using a high-dimensional white matter atlas. *Medical Imaging, IEEE Transactions on* **26**(11) (2007) 1562–1575
21. Jin, Y., Shi, Y., Zhan, L., Gutman, B.A., de Zubicaray, G.I., McMahon, K.L., Wright, M.J., Toga, A.W., Thompson, P.M.: Automatic clustering of white matter fibers in brain diffusion mri with an application to genetics. *Neuroimage* **100** (2014) 75–90
22. Filippone, M., Camastra, F., Masulli, F., Rovetta, S.: A survey of kernel and spectral methods for clustering. *Pattern recognition* **41**(1) (2008) 176–190
23. Von Luxburg, U.: A tutorial on spectral clustering. *Statistics and computing* **17**(4) (2007) 395–416